Absolute total cross sections for the photodissociation of Ar_2^+, Kr_2^+, Xe_2^+, KrN_2^+, and KrN^+ from 565 to 695 nm†

Thomas M. Miller, Joyce H. Ling, Roberta P. Saxon, and John T. Moseley*
Molecular Physics Center, Stanford Research Institute, Menlo Park, California 94025
(Received 14 January 1976)

Absolute measurements have been made of total cross sections for the photodissociation of Ar_2^+, Kr_2^+, and Xe_2^+ over the photon wavelength range 565–695 nm. A drift-tube mass-spectrometer apparatus was used with a tunable dye laser for these measurements. Calculations have been made of the bound-free Franck-Condon factors between the relevant ground and dissociating states of Ar_2^+ and a comparison is made to the photodissociation results. It is shown that the photodissociation measurements provide a sensitive test of ion-atom potential curves and that the absolute value of the transition dipole matrix element can be obtained from a match to the experimental data. In addition, we have obtained photodissociation cross sections for ArN_2^+, KrN_2^+, and KrN^+.

I. INTRODUCTION

We have made measurements of total photodissociation cross sections for several positive ions, in the wavelength range 565–695 nm. Our primary goal is to gain an understanding of the photodissociation process in the simplest case, the photodissociation of homonuclear diatomic ions, e.g.,

$$Ar_2^+ + h\nu \rightarrow Ar^+ + Ar. \quad (1)$$

For the noble-gas molecular ions we have studied (Ar_2^+, Kr_2^+, Xe_2^+), there are no strongly bound excited states and the total photodissociation cross section is expected to vary smoothly with photon wavelength. No structure characteristic of a bound excited state is expected in the cross section, such as was observed for O_3^- and CO_3^- ions by Cosby *et al.*[1,2] Rather, direct dissociation from a repulsive excited state of the ion is expected, such as was observed in the photodissociation of H_2^+, HD^+, and D_2^+ by von Busch and Dunn,[3] by van Asselt, Maas, and Los,[4] and by Ozenne *et al.*[5] Potential curves for the noble-gas ions are available from *ab initio* calculations.[6–8] In addition, experimental information on the Ar_2^+ system has been obtained in ion-atom scattering experiments by Lorents, Olson, and Conklin,[9] and by Jones, Conklin, Lorents, and Olson,[10] and by Mittmann and Weise.[11]

We also report here total photodissociation cross sections for ArN_2^+, KrN_2^+, and KrN^+, and observations regarding a few related ions.

II. APPARATUS AND EXPERIMENTAL METHOD

The apparatus used in this work has been described in detail elsewhere.[1,12] A drift-tube mass-spectrometer is utilized as the source, mass analyzer, and detector of ions of interest. The drifting ions are intersected by a laser beam ~1.5 mm before the end of the ion drift region. The laser is a jetstream dye laser pumped by a 12-W argon-ion laser. The intersection of the drifting ions and the photons takes place inside the cavity of the dye laser. The intracavity laser power is determined from the intensity of the output beam passed by the calibrated output coupler.

The total photodissociation cross section is determined from observation of the change in the parent-ion intensity as the laser beam is chopped on and off at 100 Hz. The photodissociation cross section at a particular wavelength λ is given by

$$\sigma(\lambda) = \frac{k \ln(I_0/I)}{t\Phi(\lambda)}, \quad (2)$$

where I_0 is the ion intensity with the laser off, I is the ion intensity with the laser on, $\Phi(\lambda)$ is the photon flux, t is the average time an ion spends traversing the laser beam, and k is a factor which represents the overlap between the laser beam and that portion of the ion swarm viewed by the detection system. The time t is deduced from the measured ion drift velocity. The uncertainty involved in the calculation of t has been discussed in Ref. 1 and will be dealt with in Sec. IV. The factor k is difficult to calculate accurately because the spatial distribution of photons is not accurately known, and the randomizing effect of ion-molecule collisions in the drift tube is to modify k somewhat. We choose to obtain absolute cross sections through a normalization procedure instead. The absolute photodetachment cross section for the process

$$O_2^- + h\nu \rightarrow O_2 + e \quad (3)$$

has been determined.[1,12] The details of our normalization procedure are given in Ref. 1. In the present work, we would introduce a small (3%) amount of O_2 gas into the drift tube containing the working gas (e.g., Ar), reverse the potentials on the ion source and drift tube, and make measurements on the photodetachment process (3) to determine k. As a consistency test, the working gas is then entirely replaced with O_2 and process (3) is remeasured.

The intracavity laser intensity depends on the dye being used and the photon wavelength, but was in the range 1–50 W. The ion intensity at the detector was 10^3–10^4 ions/sec. The gas pressure in the drift tube was 33 Pa (0.25 torr). The ratio of the electric field strength to the gas number density was $E/N = 5.0$ Td for most of the data (1 Townsend = 10^{-17} V cm^2). At this value of E/N the ion drift velocity is much smaller than the average thermal velocity and the ions are essentially in thermal equilibrium with gas (300 °K).[13] Our drift tube has a movable ion source which is utilized to vary the ion drift distance, a feature which allows accurate measurement of ion drift velocities and ion-molecule reaction rates, and permits tests relating to the thermalization of the internal energy of the ions (Sec. IV).

The photodissociation cross section can also be determined by observation of the photofragment ion intensity in cases where there are no competing processes producing or destroying the ions of interest. However, there is much less uncertainty in the results obtained via our usual procedure, that of observing the disappearance of parent ions. We can also operate the ion source in a pulsed mode, making time-of-flight measurements with a multichannel scaler in order to determine ion drift velocities. In most cases time-of-flight measurements (with laser-on and laser-off) and the product-ion observations enable us to identify the photodissociation products.

III. DISCUSSION OF RESULTS

A. Homonuclear diatomics

Our absolute cross sections for the photodissociation of Ar_2^+, Kr_2^+, and Xe_2^+ are given in Figs. 1–3. The photon wavelength range covered by the measurements is approximately 565–695 nm (1.78–2.18 eV). (Three laser dyes were required to cover this range in an overlapping fashion: rhodamine 6G, rhodamine B, and cresyl violet.) Attempts to observe the photodissociation of Ne_2^+ and He_2^+ were not successful, and it was found that the cross sections for these ions are smaller than 7×10^{-21} cm^2 at the photon energies used in this experiment.

Figure 4 calls attention to the large differences in the magnitude of the photodissociation cross sections for the noble-gas molecular ions. The Xe_2^+ photodissociation cross section is almost 100 times larger than that for Ar_2^+ in this wavelength range, and the Kr_2^+ results lie in between.

B. Ar_2^+ ions

Interatomic potential curves are available from ion-atom scattering data and *ab initio* calculations. We have used this information to predict the variation of the Ar_2^+ photodissociation cross section with photon wavelength. The absolute magnitude of the photodissociation cross section cannot be given without knowledge of the transition dipole moment and its variation with interatomic dis-

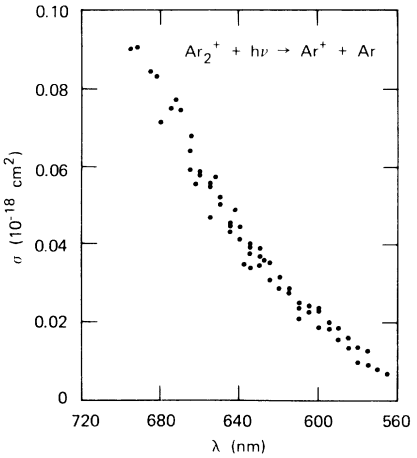

FIG. 1. Absolute cross sections for the photodissociation of Ar_2^+.

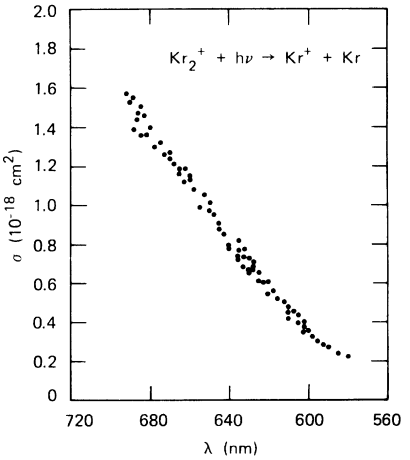

FIG. 2. Absolute cross sections for the photodissociation of Kr_2^+.

tance. However, we have assumed that the transition dipole moment is independent of internuclear separation; this assumption is reasonable in view of the very narrow (0.15 Å) range of interatomic distance dealt with here. Within this assumption, the experimental photodissociation cross section should be given by the product of the Franck-Condon factor for the transition and the square of the average value of the transition dipole moment function.

We have calculated bound-free Franck-Condon factors for the absorption transition $^2\Sigma_u^+ - {}^2\Pi_g$ for Ar_2^+, using a program provided by K. Sando.[14] The relevant potential curves are shown in Fig. 5. The Ar_2^+ potential curves considered are (a) those calculated by Gilbert and Wahl,[6] which are consistent with the elastic and inelastic scattering results of Lorents, Olson, and Conklin[9] and Jones, Conklin, Lorents, and Olson,[10] and (b) potential curves derived from ion-atom scattering data by Mittmann and Weise.[11] For case (a), the $^2\Sigma_u^+$ ground state is given by ($R > 2a_0$):

$$V(R) = 0.0459\{\exp[7.914(1 - R/4.6)] - 2\exp[3.957(1 - R/4.6)]\}, \quad (4)$$

where the energy is in hartrees, and R is in a_0. The dissociating state ($^2\Pi_g$) is given by ($R > 2a_0$)[10]:

$$V_1(R) = 112.25\exp(-1.6389R) - 7.5\exp(-1.157R). \quad (5)$$

The corresponding potentials of Mittmann and Weise are given by[11]:

$$U(R) = 0.04924\{\exp[8\rho(1 - R/4.6)] - 2\exp[4\rho(1 - R/4.6)]\}, \quad (6)$$

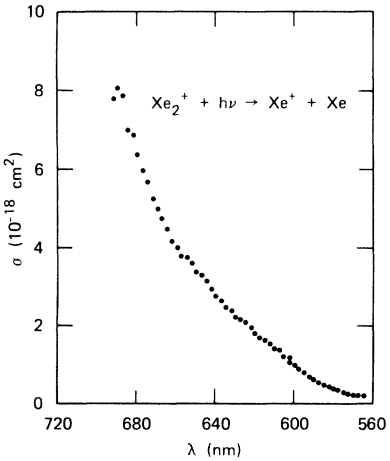

FIG. 3. Absolute cross sections for the photodissociation of Xe_2^+.

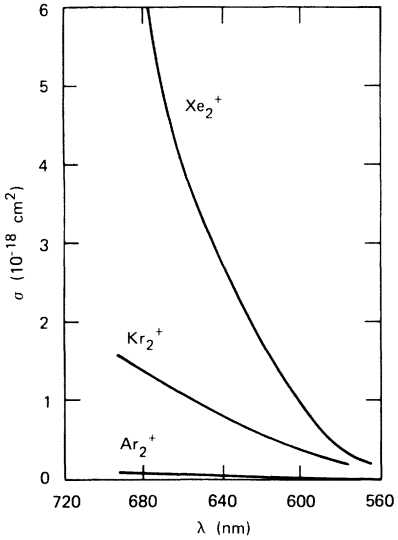

FIG. 4. Comparison of the photodissociation cross sections for Ar_2^+, Kr_2^+, and Xe_2^+. Upper limits on the photodissociation cross sections for He_2^+ and Ne_2^+ were determined, and are well below the curve shown for Ar_2^+.

where $\rho = 1$ for $R < 4.6a_0$ and $\rho = 0.95$ for $R \geq 4.6a_0$, and

$$U_1(R) = 0.011\,02\{\exp[9.86(1 - R/5.29)] - 2\exp[4.93(1 - R/5.29)]\}. \quad (7)$$

Mittmann and Weise's ground-state potential is more strongly bound than Gilbert and Wahl's, by 0.09 eV. Their excited-state potential lies below

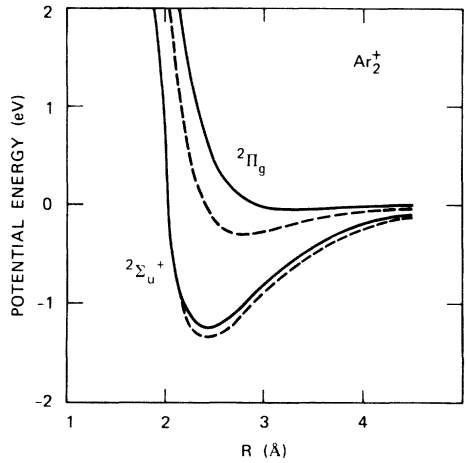

FIG. 5. Potential curves for two states of Ar_2^+. In our experiment the ion is excited by the laser radiation, from the ground $^2\Sigma_u^+$ state to the dissociating $^2\Pi_g$ state. The solid curves are from Gilbert and Wahl, Ref. 6. The dashed curves are those given by Mittmann and Weise, Ref. 11.

Gilbert and Wahl's, as shown in Fig. 5. However, the $^2\Pi_g$ potential of Mittmann and Weise, Eq. (7), is somewhat arbitrary since their experiment yields the $(^2\Pi_g, ^2\Pi_u)$ difference potential only.

The probability distribution in the lowest vibrational state of the $^2\Sigma_u^+$ potential gives the photodissociation cross section $\sigma(\lambda)$ a maximum, with a skew and width determined primarily by the shape of the repulsive $^2\Pi_g$ potential curve. At higher temperatures, $\sigma(\lambda)$ is broadened by higher vibrational levels. Our calculations included vibrational states $v = 0, 1$, and 2 with thermal weighting (300 °K). The effect of including $v = 1$ and 2 was a slight broadening of the $\sigma(\lambda)$ peak. Trial calculations included all thermally significant rotational states, but the results were found to be independent of rotational state. Subsequent calculations included $J = 1$ only. The results for Ar_2^+ photodissociation are shown in Fig. 6 for the Gilbert and Wahl potentials and for the Mittmann and Weise potentials. The $^2\Pi_g$ potentials used in our calculations are not completely repulsive. If it were possible to obtain photodissociation data at very long wavelengths ($\lambda > 900$ nm, off the scale of Fig. 6) one would expect to encounter an abrupt zero in the cross section due to excitation to a bound portion of the $^2\Pi_g$ potential of Mittmann and Weise [Eq. (7)]. The slight well of the Gilbert and Wahl $^2\Pi_g$ potential would not affect $\sigma(\lambda)$ to an observable degree. The scale for plotting the calculated cross sections is arbitrary. In Fig. 6 we have used a value for the transition dipole matrix element

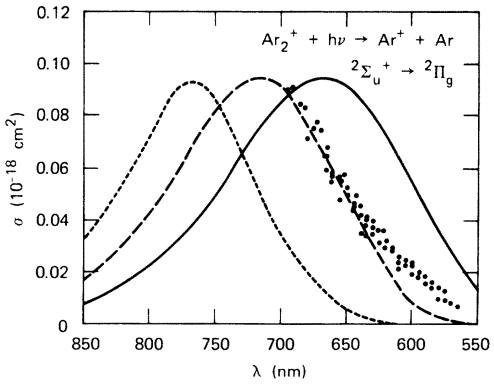

FIG. 6. Calculated photodissociation cross sections for Ar_2^+, normalized in height to effect a reasonable comparison to our experimental data. The solid curve was obtained using the Gilbert and Wahl potentials, Eqs. (4) and (5). The long-dashed curve was also obtained using Gilbert and Wahl's potentials, but with the excited-state potential, Eq. (5), multiplied by 0.8. The short-dashed curve was obtained using the potentials given by Mittmann and Weise, Eqs. (6) and (7). The points are our data.

(squared) of ~0.009 a.u. The calculated and experimental cross sections obviously peak at different wavelengths. However, the potential curves are not expected to be accurate to better than ~0.1 eV, and shifts in the potential curves on this order can produce agreement with our data. To illustrate the magnitude of the adjustment required, we have used the Gilbert and Wahl $^2\Pi_g$ potential multiplied by 0.8 in the Franck-Condon calculation, and find a result shown as the long-dashed curve in Fig. 6. This lowers the curve by about 0.18 eV in the region relevant to our experiment. Definitive adjustments of the potential curves are not warranted until photodissociation data have been obtained over a wider photon wavelength range which includes the maximum in $\sigma(\lambda)$. Still, the adjustments will not be unique, since the present experiment is sensitive primarily to the difference between the two potential curves. (We are constructing a crossed-beams apparatus which will allow us to make detailed observations of the photofragment ions in order to extract more information about the potentials.)

It should be noted that the present photodissociation experiment and ion-atom scattering experiments provide complementary information. The scattering experiments[9–11] are sensitive to the $^2\Sigma_u^+$ well depth and to the $(^2\Sigma_u^+, ^2\Sigma_g^+)$ and $(^2\Pi_g, ^2\Pi_u)$ *difference* potentials, while our photodissociation work determines the $(^2\Sigma_u^+, ^2\Pi_g)$ *difference* potential [and the $(^2\Sigma_u^+, ^2\Sigma_g^+)$ *difference* potential at much shorter wavelengths]. The photodissociation experiments provide a much more sensitive result because of the optical resolution and precision which can be rountinely achieved, but it is difficult to cover a large energy range. By combining results from these photodissociation experiments, ion-atom scattering, and the crossed-beams photofragment spectroscopy experiments, it should be possible to construct quite accurate potentials for molecular ions.

C. Noble-gas–nitrogen ions

Data for ArN_2^+, shown in Fig. 7, were obtained in a 92%-N_2, 8%-Ar mixture. It was not possible to determine the dissociation channel(s) because of interference from the photodissociation of N_4^+ and Ar_2^+ ions present in the drift tube. Teng and Conway[15] have measured the bond energy $D(Ar\text{-}N_2^+)$ to be 1.07 eV using a high-pressure mass spectrometer.

The ion KrN_2^+ was detected at the rate of ~2000 ions/sec in N_2 gas to which a trace (~0.05%) of Kr gas was added. Photodissociation was seen to proceed as

$$KrN_2^+ + h\nu \rightarrow Kr^+ + N_2 \ , \qquad (8)$$

and the results are given in Fig. 8.

As more Kr gas was added, the triatomic (KrN_2^+) ion intensity dropped and the diatomic (KrN^+) ion intensity became strong enough to permit photodissociation measurements to be made. It was found that

$$KrN^+ + h\nu \rightarrow Kr^+ + N \ , \qquad (9)$$

and the cross sections are presented in Fig. 9. For these measurements the gas mixture was 98.4% N_2 and 1.6% Kr. If further additions of Kr gas were made, most of the ionization was taken up by the formation of Kr_2^+ ions.

For our work with nitrogen–noble-gas mixtures the cross sections were normalized through our Kr_2^+ and Ar_2^+ results, rather than directly to O_2^- photodetachment.

D. Other ions

We have attempted the formation of other ions in the drift tube for which we felt photodissociation would be interesting. This study is considered to be a preliminary survey of photodissociation of noble-gas ions and in most of the cases where problems were encountered, no lengthy attempts were made to solve them. Thus, successful measurements can probably be made on most species (where photodissociation is physically possible) if a more serious effort is warranted.

In Xe-N_2 gas mixtures XeN^+ ions were observed. An upper limit of 10^{-20} cm^2 was determined for the photodissociation cross section of XeN^+ at 600 nm.

Because of the use of oxygen in noble-gas excimer lasers, we attempted to produce ions such as XeO^+ and XeO_2^+. However, even a trace of O_2 gas added to Xe or Kr gas in the drift tube resulted in most of the ionization appearing as O_2^+. In Kr gas we were able to generate weak currents of KrO^+ and KrO_2^+, which were inadequate for photodissociation measurements.

We also used noble-gas mixtures in order to create such ions as $KrAr^+$ or $XeKr^+$. Small amounts of $KrAr^+$ could be made, and larger amounts of $XeKr^+$ were possible. An upper limit for the photodissociation of $KrAr^+$ was determined to be 8×10^{-21} cm^2 at 640 nm. No definitive results for $XeKr^+$ have been obtained. $XeKr^+$ was observed to photodissociate at 600 nm with a cross section on the order of 2×10^{-19} cm^2.

ArH^+ ions were observed in Ar-H_2 gas mixtures, and an upper limit to the photodissociation cross section is 10^{-19} cm^2 at 600 nm. Very small amounts of Ar_2H^+ ions were also observed.

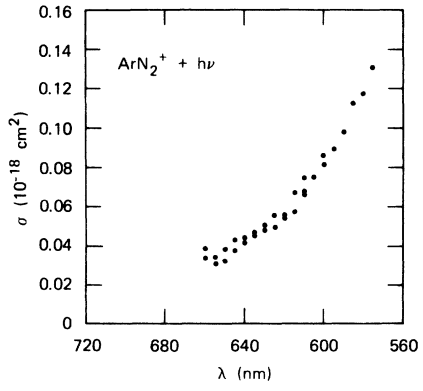

FIG. 7. Absolute cross sections for the photodissociation of ArN_2^+. It was not possible in this case to determine the dissociation channel(s).

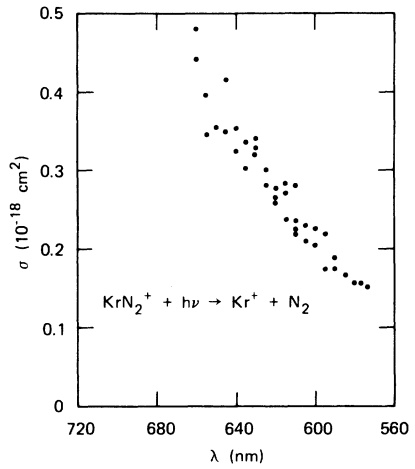

FIG. 8. Absolute cross sections for the photodissociation of KrN_2^+.

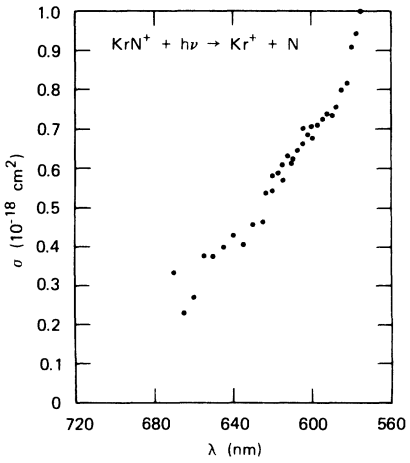

FIG. 9. Absolute cross sections for the photodissociation of KrN^+.

IV. ANALYSIS OF UNCERTAINTIES

The statistical uncertainty in our results is primarily that in measuring $\ln(I_0/I)$ in Eq. (2) and is typically 6%, depending on the intensity of the ion species studied and the laser power at a given wavelength. The uncertainty in the absolute cross section magnitude is determined by the quality of our normalization procedure. By making measurements both with the ion of interest (e.g., Ar_2^+) and with the standard (O_2^-) we eliminate the need to know k in Eq. (2) and we eliminate the need to determine the photon flux absolutely. The time t that the ions spend in the laser beam also appears in Eq. (2); in normalizing to O_2^- we require the ratio of the average velocity of O_2^- to that for the ion of interest. The uncertainty in the ratio of velocities has been discussed in Ref. 1. However, in the present case we are operating at higher pressures than were used previously and the use of the ratio of the ion drift velocities should be an accurate measure of the inverse ratio of the transit times. We ascribe a 25% uncertainty to the normalization, including 12% associated with the O_2^- results used as the standard.[1]

We used ion mobilities from Ref. 13 to obtain drift velocities, except for Kr_2^+ and Xe_2^+, where we used more recently measured mobilities (0.995 and 0.616 $cm^2/V\,sec$, respectively).[16] For ions where no measured mobilities exist (e.g., ArN_2^+, KrN_2^+, KrN^+) we used measured values for related ions, adjusted to the proper ion mass.[13]

We made a number of consistency checks on the data. In cases such as reaction (1) where there are no competing processes, we checked the shape of the $\sigma(\lambda)$ curve by observation of the appearance of the product ions when the laser is chopped on. We also checked the photodissociation signal as the reactant ion intensity was varied and as the laser power was varied. If both of these factors were sufficiently low, no effect was observed on the cross section. For high levels of the reactant ion intensity, mutual repulsion effects can be seen. For higher laser power levels effects can occur if the reactant ion intensity is large or if the fraction of ions dissociated is large. For example, the fraction of Ar_2^+ ions dissociated was never greater than 3.6% in this work, and no nonlinear effects of laser power were observed even at the largest available power level of 50 W. With Xe_2^+, we could dissociate 65% of the ions and did observe strong laser power effects above a few watts of laser power. All data presented here were, of course, obtained at low enough power levels that the cross section remained constant as the power was varied.

As an additional test, we increased the electric field strength in the drift tube, which increases the ion drift velocity [or decreases t in Eq. (2)]. In calculating the normalized cross sections, such an increase in the ion velocities should cancel. Indeed, the cross sections were observed to remain constant as long as the drift velocities were much smaller than thermal velocities, such that vibrational excitations of the ions was not possible.

V. CONCLUSIONS

We have made measurements of total photodissociation cross sections for noble-gas diatomic ions and for ions in nitrogen–noble-gas mixtures for photon wavelengths in the range 565–695 nm. The results are presented in Figs. 1–4 and 7–9. We have made calculations of the photodissociation cross section in a typical case, reaction (1), for which potential curves are available. We have shown that small adjustments of these potential curves can produce agreement with the shape of the measured $\sigma(\lambda)$ curve, although the experimental data must be extended to longer wavelengths for a more definitive match to be made. Nevertheless, it is clear that measurements of photodissociation cross sections can be a sensitive test of proposed ion-atom potential curves, and that the absolute value of the transition dipole matrix element can be obtained as well.

ACKNOWLEDGMENTS

We would like to express our appreciation to Professor Kenneth Sando for providing the computer program used for the calculations of Franck-Condon overlap factors. We also acknowledge valuable discussions with Dr. David L. Huestis, Dr. James R. Peterson, and Dr. Philip C. Cosby of SRI during the course of this research.

---

†Supported by the National Science Foundation under Grant No. MPS75-10085.

*Present address: Laboratoire des Collisions Ioniques, Universite de Paris-Sud, 91405 Orsay, France.

[1]P. C. Cosby, R. A. Bennett, J. R. Peterson, and J. T. Moseley, J. Chem. Phys. 63, 1612 (1975).

[2]P. C. Cosby and J. T. Moseley, Phys. Rev. Lett. 34, 1603 (1975).

[3]F. von Busch and G. H. Dunn, Phys. Rev. A 5, 1726 (1972).

[4]N. P. F. B. van Asselt, J. G. Maas, and J. Los, Chem. Phys. 5, 429 (1974); Chem. Phys. Lett. 24, 555 (1974).

[5]J. B. Ozenne, D. Pham, and J. Durup, Chem. Phys. Lett. 17, 422 (1972); J. B. Ozenne, J. Durup, R. W. Odom, C. Pernot, A. Tabche-Fouhaile, and M. Tadjeddine, VII[e] Colloque National sur la Physique des Collisions Atomiques et Electroniques, Bordeaux, France, 1975 (unpublished).

[6]T. L. Gilbert and A. C. Wahl, J. Chem. Phys. 55, 5247 (1971).

[7]R. Mulliken, J. Chem. Phys. 52, 5170 (1970).

[8]V. Sidis, M. Barat, and D. Dhuicq, J. Phys. B 8, 474 (1975).

[9]D. C. Lorents, R. E. Olson, and G. M. Conklin, Chem. Phys. Lett. 20, 589 (1973).

[10]P. R. Jones, G. M. Conklin, D. C. Lorents, and R. E. Olson, Phys. Rev. A 10, 102 (1974).

[11]H.-U. Mittmann and H.-P. Weise, Z. Naturforsch. 29a, 400 (1974).

[12]J. T. Moseley, P. C. Cosby, R. A. Bennett, and J. R. Peterson, J. Chem. Phys. 62, 4826 (1975).

[13]E. W. McDaniel and E. A. Mason, *The Mobility and Diffusion of Ions in Gases* (Wiley, New York, 1973).

[14]K. Sando, University of Iowa (private communication).

[15]H. H. Teng and D. C. Conway, J. Chem. Phys. 59, 2316 (1973). These authors caution that it is difficult to state the uncertainty in their result for $D(\mathrm{Ar}\text{-}N_2^+)$ because of the uncertainty in $D(N_2\text{-}N_2^+)$ on which the data analysis depends.

[16]H. Helm (private communication).